Vol 15 No 8, August 2006
1009-1963/2006/15(08)/1738-08

Chinese Physics

© 2006 Chin. Phys. Soc.
and IOP Publishing Ltd

Isospin- and momentum-dependent interaction in isospin-dependent quantum molecular dynamics*

Liu Jian-Ye(刘建业)[a)b)d)], Guo Wen-Jun(郭文军)[c)], Ren Zhong-Zhou(任中洲)[c)d)], Xing Yong-Zhong(邢永忠)[a)d)], Zuo Wei(左　维)[b)d)], and Lee Xi-Guo(李希国)[b)d)]

[a)] *Department of Physics, Tianshui Normal College, Gansu, Tianshui* 741000, *China*
[b)] *Institute of Modern Physics, Chinese Academy of Sciences, Lanzhou* 730000, *China*
[c)] *Department of Physics, Nanjing University Nanjing* 210008, *China*
[d)] *Center of Theoretical Nuclear Physics, National Laboratory of Heavy Ion Accelerator, Lanzhou* 730000, *China*

(Received 8 September 2005; revised manuscript received 18 April 2006)

An isospin-dependent quantum molecular dynamical model (IQMD) is developed, with the isospin degree of freedom in the momentum-dependent interaction(MDI) included in IQMD, to obtain an isospin- and momentum-dependent interaction (IMDI) in IQMD. We investigate the effect of IMDI on the isospin fractionation ratio and its dynamical mechanism in the intermediate energy heavy ion collisions. It is found that the IMDI induces the significant reductions in the isospin fractionation ratio for all of beam energies, impact parameters, neutron–proton ratios and mass number of colliding systems. However, the strong dependence of isospin fractionation ratio on the symmetrical potential is preserved, with the isospin degree of freedom included in the MDI, i.e. the isospin fractionation ratio is still a good probe for extracting the information about the equation of state of isospin asymmetrical nuclear matter.

Keywords: heavy ion collision, isospin fractionation ratio, isospin and momentum dependent interaction, isospin effect

PACC: 2570

1. Introduction

The study of the isospin effect in intermediate energy heavy ion collisions can obtain the information of the in-medium nucleon–nucleon (N–N) cross section and isospin-dependent mean field. Therefore, several interesting isospin effects in heavy ion collisions have been explored both experimentally and theoretically over the last few years.[1−31] Li and Di Toro *et al* studied the isospin fractionation in the intermediate energy heavy ion collisions in recent years.[14,15,19,30] We investigated also the isospin effects of isospin-dependent mean field and in-medium N–N collisions on the observable in the intermediate energy heavy ion collisions separately.[20−29,31] The effects of momentum-dependent interaction on the observable in the heavy ion collisions have been studied for many years. However, the isospin dependence of MDI and its effect on the collision dynamics have not been studied yet. Recently Das Gupta *et al* investigated the isospin dependence of momentum-dependent potential in the asymmetric nuclear matter and gave a formula of symmetrical potential with momentum interaction for Boltzmann–Uehling–Uhlenbeck (BUU) calculations and heavy ion collisions induced by neutron-rich nuclei.[32,33] However, the isospin dependence of MDI in the IQMD has not been taken into account. This work aims to develop the IQMD, with an isospin degree of freedom in the MDI included in IQMD, to obtain an IMDI for the practical calculation in IQMD. A short report of this study can be found in Ref.[34]. In this paper we use IQMD with IMDI to investigate systematically the effects of IMDI on the isospin fractionation ratio and its dynamical mechanism in the intermediate energy heavy ion collisions for different beam energies, different impact parameters, different neutron–proton ratios and mass numbers of colliding systems. It is found that IMDI brings an important isospin effect to the isospin fractionation ratio for all of entrance channel conditions studied.

*Project supported by the State Key Program of Basic Research of China(Grant No G2000077400), the Major program of the National Natural Science Foundation of China (Grant Nos 10435080 and 105350101), the National Natural Science Foundation of China (Grant Nos 10447006, 10575075, 10125521 and 10447113), the Knowledge Innovation Program of the Chinese Academy of Sciences (Grant No KJCX2-SW-N02), Jiangsu Planned Projects for Postdoctoral Research Funds and China Postdoctoral Science Foundation.

2. IQMD model with IMDI

2.1. IQMD model with MDI

It is known that quantum molecular dynamics (QMD)[35,36] contains two dynamical ingredients: density-dependent mean field and in-medium N–N collision cross section. In order to describe isospin effects appropriately, QMD should be modified properly, for example, the density-dependent mean field should contain correct isospin terms. This includes the symmetrical potential and the Coulomb potential. The in-medium N–N cross section should be different from the cross sections of neutron–neutron (proton–proton) and neutron–proton collisions, in which Pauli blocking should be counted by distinguishing between neutrons and protons. In addition, the initial condition of the ground state of two colliding nuclei should also contain isospin information, such as the initial density distributions of the colliding nuclei in IQMD model, which are obtained from the calculations of the Skyrme–Hartree–Fock with the parameter set SKM*,[37] and the starting code of IQMD, which is used to determine the ground state properties of the colliding nuclei, for example, the binding energies and root mean square (RMS) radii, which are consistent with the experimental data. By calculating the above quantities the interaction potential in IQMD is determined as follows:

$$U(\rho) = U^{\rm Sky} + U^{\rm Coul} + U^{\rm sym} + V^{\rm Yuk} + V^{\rm MDI} + V^{\rm Pauli}, \tag{1}$$

where $U^{\rm Sky}$ is Skyrme potential

$$U^{\rm Sky} = \alpha(\frac{\rho}{\rho_0}) + \beta(\frac{\rho}{\rho_0})^{\gamma}. \tag{2}$$

$V^{\rm Yuk}$ and $V^{\rm Pauli}$ are Yukawa and Pauli interactions, which are given as follows:

$$V^{\rm Yuk} = t_3 \exp(\frac{|\boldsymbol{r}_1 - \boldsymbol{r}_2|}{m})/\frac{|\boldsymbol{r}_1 - \boldsymbol{r}_2|}{m}, \tag{3}$$

$$V^{\rm Pauli} = V_{\rm p}(\frac{\hbar}{p_0 q_0})^3 \exp(-\frac{(\boldsymbol{r}_i - \boldsymbol{r}_j)^2}{2q_0^2} - \frac{(\boldsymbol{p}_i - \boldsymbol{p}_j)^2}{2p_0^2})\delta_{p_i p_j}, \tag{4}$$

with

$$\delta_{p_i p_j} = \begin{cases} 1 \text{ for neutron–neutron or proton–proton,} \\ 0 \text{ for neutron–proton.} \end{cases}$$

$U^{\rm Coul}$ is the Coulomb potential. $U^{\rm sym}$ is the symmetrical potential. In this paper, two different forms of $U^{\rm sym}$ have been used:[1,2]

$$U_1^{\rm sym} = cF_1(u)\delta\tau_z, \tag{5}$$

$$U_2^{\rm sym} = cF_2(u)[\delta\tau_z - \frac{1}{4}\delta^2] \tag{6}$$

with

$$\tau_z = \begin{cases} 1, & \text{for neutron,} \\ -1, & \text{for proton,} \end{cases}$$

where c is the strength of symmetrical potential with a value of 32MeV. $F_1(u) = u$ and $F_2(u) = u^{1/2}$ and $u = \rho/\rho_0$. δ is the relative neutron excess $\delta = (\rho_{\rm n} - \rho_{\rm p})/(\rho_{\rm n} + \rho_{\rm p}) = (\rho_{\rm n} - \rho_{\rm p})/\rho$. ρ, ρ_0, $\rho_{\rm n}$ and $\rho_{\rm p}$ are the total, normal, neutron and proton densities, respectively. The curvatures $K_{\rm sym}$ of $U_1^{\rm sym}$ and $U_2^{\rm sym}$ are -27 MeV and -69 MeV respectively. $V^{\rm MDI}$ is momentum-dependent interaction[36]

$$V^{\rm MDI} = t_4 \ln^2[t_5(\boldsymbol{p}_1 - \boldsymbol{p}_2)^2 + 1]\frac{\rho}{\rho_0}. \tag{7}$$

An empirical density-dependent expression of the in-medium N–N cross section[38]

$$\sigma_{\rm NN}^{\rm med} = (1 + \alpha\frac{\rho}{\rho_0})\sigma_{\rm NN}^{\rm free} \tag{8}$$

is used. In the above equation the parameter α=-0.2 is found to reproduce the data of flow. Here $\sigma_{\rm NN}^{\rm free}$ is the experimental nucleon–nucleon (N–N) collision cross section.[39] We make use of Eq.(8) to obtain the medium effect in the N–N collisions. The main physics and the relevant numerical calculation in the IQMD model can be found in Refs.[1,2,35-37,40].

2.2. IMDI

The momentum-dependent interaction without isospin dependence in IQMD is shown by Eq.(7) that is extracted from optical potential.[36] In order to include the isospin effects of MDI on the observable we insert an isospin degree of freedom into the MDI to obtain an IMDI. It should be different from that for neutrons or protons. In this case, IQMD includes an IMDI for the neutrons

$$V_{\rm n}^{\rm IMDI}(\rho, k_{\rm n}, p) = t_4 \ln^2[t_5(\boldsymbol{p}_{\rm n} - \boldsymbol{p}_{\rm n}^{''})^2 + 1]C_{\rm nn}\frac{\rho_{\rm n}}{\rho_0} + t_4 \ln^2[t_5(\boldsymbol{p}_{\rm n} - \boldsymbol{p}_{\rm p})^2 + 1]C_{\rm np}\frac{\rho_{\rm p}}{\rho_0}, \tag{9}$$

and that for the protons

$$V_{\rm p}^{\rm IMDI}(\rho,k_{\rm p},n)=t_4\ln^2[t_5(\boldsymbol{p}_{\rm p}-\boldsymbol{p}_{\rm p}^{''})^2+1]C_{\rm pp}\frac{\rho_{\rm p}}{\rho_0}+t_4\ln^2[t_5(\boldsymbol{p}_{\rm p}-\boldsymbol{p}_{\rm n})^2+1]C_{\rm pn}\frac{\rho_{\rm n}}{\rho_0}. \tag{10}$$

Here, p on the left-hand side and $\boldsymbol{p}_{\mathbf{n}}^{''}$ on the right-hand side of bracket in Eq.(9) represent proton-symbol and the momenta of other neutrons respectively. Similarly n on the left-hand side and $\boldsymbol{p}_{\rm p}^{''}$ on the right-hand side bracket in Eq.(10)represent the neutron-symbol and the momenta of other protons respectively. In the above equation, ρ=$\rho_{\rm n}+\rho_{\rm p}$, $\boldsymbol{p}_{\rm n}=\hbar\boldsymbol{k}_{\rm n}$ and $\boldsymbol{p}_{\rm p}=\hbar\boldsymbol{k}_{\rm p}$. The first term and second term on the right-hand sides of Eq.(9) and Eq.(10) refer to the interactions between like nucleons and unlike nucleons, respectively. For example the IMDI of neutron, i.e. $V_{\rm n}^{\rm IMDI}(\rho,k_{\rm n},p)$ should include the interactions between a neutron with $p_{\rm n}$ and the other neutrons with $p_{\rm n}^{''}$ and between a neutron with $p_{\rm n}$ and all of protons with $p_{\rm p}$. Similarly, $V_{\rm p}^{\rm IMDI}(\rho,k_{\rm p},n)$ should include the interactions between a proton with $p_{\rm p}$ and the other protons with $p_{\rm p}^{''}$ and between a proton with $p_{\rm p}$ and all of neutrons with p_n. Finally, we can obtain an isospin- and momentum-dependent interaction

$$V_\tau^{\rm IMDI}(\rho,k_\tau,\tau')=t_4\ln^2[t_5(\boldsymbol{p}_\tau-\boldsymbol{p}_{\tau''})^2+1]C_{\tau\tau}\frac{\rho_\tau}{\rho_0}+t_4\ln^2[t_5(\boldsymbol{p}_\tau-\boldsymbol{p}_{\tau'})^2+1]C_{\tau\tau'}\frac{\rho_{\tau'}}{\rho_0}, \tag{11}$$

where $\rho=\rho_\tau+\rho_{\tau'}$ and $\boldsymbol{p}_{\boldsymbol{\tau}}=\hbar\boldsymbol{k}_{\boldsymbol{\tau}}$. Similarly, τ' on the left-hand side and $\boldsymbol{p}_{\boldsymbol{\tau}}^{''}$ on the right-hand side of the bracket of Eq.(11) represent nucleon τ'-symbol and the momenta of the other nucleons $\tau^{''}$ respectively. In this paper, we define $V^{\rm MDI}\equiv V^{\rm MDI}(\rho,k)\equiv$ MDI and $V^{\rm IMDI}\equiv V_\tau^{\rm IMDI}(\rho,k,\tau')\equiv$ IMDI. Here $C_{\rm nn}=C_{\rm pp}=C_{\tau\tau}$ and $C_{\rm np}=C_{\rm pn}=C_{\tau\tau'}$. In the above, $\tau\neq\tau'$. The one-body potential is given by

$$U_\tau\equiv U_\tau(\rho,k,\delta)=U^{\rm Sky}+U_\tau^{\rm IMDI}+U^{\rm sym}, \tag{12}$$

where $U^{\rm Sky}\equiv U^{\rm Sky}(\rho)$ is shown by Eq.(2) and $U^{\rm sym}\equiv U^{\rm sym}(\rho,\delta,\tau)$ is given by Eqs.(5) or (6), and then we have

$$U_\tau^{\rm IMDI}=\Sigma_{\tau''}t_4\ln^2[t_5(\boldsymbol{p}_{\boldsymbol{\tau}}-\boldsymbol{p}_{\tau''})^2+1]C_{\tau\tau}\frac{\rho_\tau}{\rho_0}+\Sigma_{\tau'}t_4\ln^2[t_5(\boldsymbol{p}_{\boldsymbol{\tau}}-\boldsymbol{p}_{\tau',})^2+1]C_{\tau\tau'}\frac{\rho_{\tau'}}{\rho_0}. \tag{13}$$

The summations on the right-hand side of Eq.(13) are taken only for the momentum of nucleon. $C_{\tau\tau}$ and $C_{\tau\tau'}$ are determined by the correspondence between the above one-body potential $U_\tau(\rho,k,\delta)$ (thick lines) and the one-body Gogny potential (thin lines)[26] as a function of momentum k for neutron (solid line) and proton (dashed line) in a cold matter as shown in Fig.1 respectively. The one-body Gogny potential is taken from the calculation of effective Gogny interaction based on the many-body theory. From the above correspondence the values of parameters $C_{\tau\tau}=0.5$ and $C_{\tau\tau'}=1.5$ are obtained. These values reveal that the neutron–proton correlation is stronger than that of neutron–neutron or proton–proton.

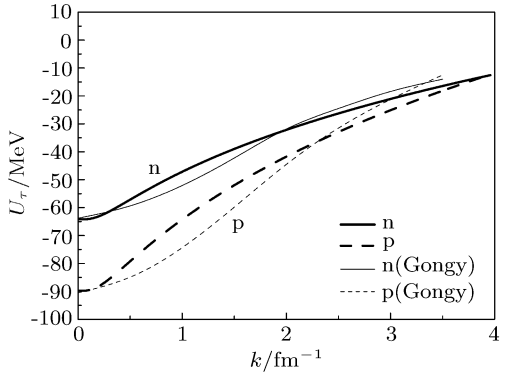


Fig.1. The correspondence between one-body potential $U_\tau(\rho,k,\delta)$ and one-body Gogny potential as a function of momentum k in cold matter.

From Fig.1 it is clear that the neutron poten-

tial is repulsive and the proton potential is attractive, compared with the potential with isospin-independent MDI.

The starting code of IQMD with IMDI is also used to determine the ground state properties of the colliding nuclei, such as the binding energies and the RMS radii, which are consistent with the experimental data. During the above starting calculation the parameters of the interaction potentials with MDI and IMDI in IQMD are given in Table 1.

Table 1. The parameters of the interaction potentials with IMDI and MDI in IQMD.

	$C_{\tau\tau}$	$C_{\tau\tau'}$	α /MeV	β /MeV	γ	t_3 /MeV	m /fm	t_4 /MeV	t_5 /(c^2/MeV^2)	$V_{\rm p}$ /MeV	p_0 /(MeV/c)	q_0 /fm
MDI	1.0	1.0	-390	320	1.14	7.5	0.8	1.57	10^{-3}	30	400	5.64
IMDI	0.5	1.5	-397	320	1.14	7.5	0.8	1.57	10^{-3}	30	400	5.64

3. Results and discussions

It is known that $(N/Z)_{\rm nucl}/(N/Z)_{\rm frag}$ for a neutron-rich system depends sensitively on the symmetrical potential and weakly on the N–N cross section.[23,25] Therefore, $(N/Z)_{\rm nucl}/(N/Z)_{\rm frag}$ is calculated for different symmetrical potentials $U_1^{\rm sym}$ and $U_2^{\rm sym}$ with the same N–N cross sections $\sigma^{\rm iso}$. Here an isospin-dependent N–N cross section in the medium is determined by $\sigma^{\rm iso}$. $\sigma^{\rm iso}$ indicates $\sigma_{\rm np} \geq \sigma_{\rm nn} = \sigma_{\rm pp}$. And $\sigma_{\rm np}$, $\sigma_{\rm nn}$ and $\sigma_{\rm pp}$ are the neutron–proton, neutron–neutron and proton–proton cross sections in the medium shown by Eq.(8) respectively.

3.1. The dependences of $(N/Z)_{\rm nucl}/(N/Z)_{\rm frag}$ on the neutron–proton ratio of colliding system for MDI and IMDI

The isospin fractionation ratio $(N/Z)_{\rm nucl}/(N/Z)_{\rm frag}$ in this paper is measured by the ratio between the neutron–proton ratio of the nucleon emissions $(N/Z)_{\rm nucl}$ and that of the fragment emissions $(N/Z)_{\rm frag}$. Here the fragments include all of fragments with the charge number $z \geq 2$, because the isospin fractionation ratio $(N/Z)_{\rm nucl}/(N/Z)_{\rm frag}$ depends on both the mass and the neutron–proton ratio of colliding system. In this case, if we investigate the dependence of $(N/Z)_{\rm nucl}/(N/Z)_{\rm frag}$ on the neutron–proton ratio of system, the mass number of system should be fixed. In this way, we can maximize the dependence of $(N/Z)_{\rm nucl}/(N/Z)_{\rm frag}$ on the neutron–proton ratio of system and minimize the effect of the system mass number on it. Similarly, if we investigate the dependence of $(N/Z)_{\rm nucl}/(N/Z)_{\rm frag}$ on the mass number of system, the neutron–proton ratio of system should be fixed.

Figure 2 shows the $(N/Z)_{\rm nucl}/(N/Z)_{\rm frag}$ at freeze-out time as a function of the neutron–proton ratio of colliding system with MDI and IMDI for the reactions ^{94}Kr +^{94} Kr, ^{94}Zr +^{94} Zr, ^{94}Mo +^{94} Mo and ^{94}Ru +^{94} Ru at a beam energy of 50 MeV/nucleon and an impact parameter of 2.0 fm. The mass numbers of the four colliding systems are the same, A=$A_{\rm p}$ + $A_{\rm t}$=188. The freeze-out time is 300 fm/c because the $(N/Z)_{\rm nucl}/(N/Z)_{\rm frag}$ arrives at a saturation value in more than about 150 fm/c. The neutron–proton ratios of the four systems are listed in Table 2.

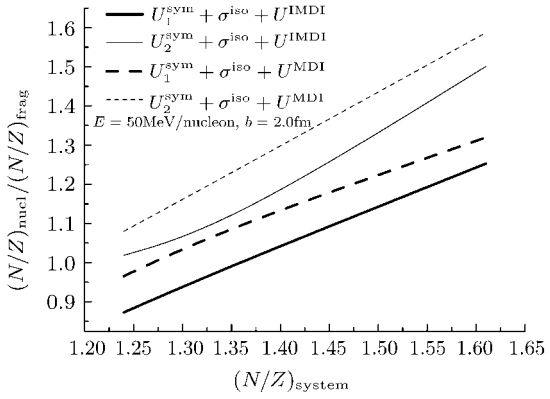


Fig.2. The $(N/Z)_{\rm nucl}/(N/Z)_{\rm frag}$ as a function of the neutron–proton ratio of system for four reactions with the same mass number A=A_1 + A_2=188.

Table 2.the neutron–proton ratios of four colliding systems.

system	^{94}Kr +^{94} Kr	^{94}Zr +^{94} Zr	^{94}Mo +^{94} Mo	^{94}Ru +^{94} Ru
N/Z	1.61	1.35	1.24	1.14

Clearly the IMDI causes $(N/Z)_{\rm nucl}/(N/Z)_{\rm frag}$ to significantly reduce from two dashed lines with MDI to two corresponding solid lines with IMDI for all of colliding systems here. From Fig.2 it is also clear that the gap between two solid lines with IMDI for different symmetrical potentials $U_1^{\rm sym}$ and $U_2^{\rm sym}$ is approximately the same in magnitude as that between two dashed lines with MDI for the same symmetrical potentials. This means that the strong dependence of $(N/Z)_{\rm nucl}/(N/Z)_{\rm frag}$ on the symmetrical potential is preserved, with the isospin degree of freedom of MDI included. We also find that the isospin fractionation ratio, $(N/Z)_{\rm nucl}/(N/Z)_{\rm frag}$ increases obviously with the enhancement of the neutron–proton ratio of system for IMD and IMDI. Because the symmetrical potential for the neutron-rich system is stronger than that of neutron-deficient system due to a larger relative neutron excess $\delta =(\rho_{\rm n}-\rho_{\rm p})/(\rho_{\rm n}+\rho_{\rm p})=(\rho_{\rm n}-\rho_{\rm p})/\rho$ for the neutron-rich system (see Eq.(5) and Eq.(6)). In this case, the neutron-rich system causes more neutrons to be emitted because the symmetrical potential is the repulsive for neutrons and attractive for protons than the neutron-deficient colliding system that leads to the reduction in $(N/Z)_{\rm nucl}$. However, the neutron–proton ratio of fragment emissions, i.e. $(N/Z)_{\rm frag}$, decreases with the increase of the neutron–proton ratio of system due to the charge number conservation of colliding system. Finally the ratio between them, $(N/Z)_{\rm nucl}/(N/Z)_{\rm frag}$, increases with the increase of neutron–proton ratio of system for MDI and IMDI. From Fig.2 it is also seen that the $(N/Z)_{\rm nucl}/(N/Z)_{\rm frag}$ is larger than 1.0 for the neutron-rich system ^{94}Kr +^{94} Kr for MDI and IMDI. This means the neutron-rich gas phase and the neutron-deficient liquid phase compared with the neutron-proton ratio of the colliding system. However, for the neutron-deficient colliding systems, such as, ^{94}Mo +^{94} Mo and ^{94}Ru +^{94} Ru, the values of $(N/Z)_{\rm nucl}/(N/Z)_{\rm frag}$ reduce gradually to less than 1.0 with the decrease of the neutron–proton ratio of the colliding system for IMD and IMDI. It reveals the neutron-deficient gas phase and neutron-rich liquid phase because the excited primary neutron-deficient fragment decays to the stable neutron-rich one towards the β stable line. In this case, $(N/Z)_{\rm frag}$ increases in the isospin fractionation process compared with the neutron–proton ratio of the neutron-deficient colliding system, where $(N/Z)_{\rm nucl}$ has to be the neutron-deficient one due to the charge number conservation of colliding system. Finally the ratio between them, $(N/Z)_{\rm nucl}/(N/Z)_{\rm frag}$ reduces gradually to less than 1.0 with the decrease of neutron–proton ratio of the system.

3.2. The dependences of $(N/Z)_{\rm nucl}/(N/Z)_{\rm frag}$ on the mass number of the system for MDI and IMDI

Figure 3 shows the $(N/Z)_{\rm nucl}/(N/Z)_{\rm frag}$ for MDI and IMDI as a function of mass number of system at a beam energy of 50 MeV/nucleon and an impact parameter of 2.0 fm. There are three neutron-rich colliding systems: ^{44}Ar +^{44} Ar,^{89}Kr +^{89} Kr and ^{124}Sn +^{124} Sn. The corresponding neutron–proton ratios are 1.44, 1.47 and 1.48 respectively, i.e. the neutron–proton ratios for three systems are approximately same. In this case, the effect of mass number of colliding system on $(N/Z)_{\rm nucl}/(N/Z)_{\rm frag}$ can be maximized by minimizing the effect of the system neutron–proton ratio on it. The different symmetrical potentials $U_1^{\rm sym}$ and $U_2^{\rm sym}$ with the same N–N cross sections $\sigma^{\rm iso}$ for MDI and IMDI are calculated. The symbols and the meanings of the four lines in Fig.3 are the same as those in Fig.2. It is clear that the IMDI causes the $(N/Z)_{\rm nucl}$ /$(N/Z)_{\rm frag}$ to significantly reduce from two dashed lines with MDI to two corresponding solid lines with IMDI for all of colliding systems. However, the strong dependence of $(N/Z)_{\rm nucl}$ / $(N/Z)_{\rm frag}$ on the symmetrical potential for all neutron-rich systems is preserved, with the isospin effect of MDI included, because the gap between two solid lines with IMDI for different symmetrical potentials $U_1^{\rm sym}$ and $U_2^{\rm sym}$ is approximately the same as that between two dashed lines with MDI for the same symmetrical potentials. From Fig.3 we can see that $(N/Z)_{\rm nucl}/(N/Z)_{\rm frag}$ decreases with the increase of the mass number of colliding system because the system density decreases with increase of the mass number of colliding system as shown in Fig.4, in which the system density for ^{44}Ar +^{44} Ar (solid line) is higher than that for ^{89}Kr+^{89}Kr (dashed line) or ^{124}Sn+^{124}Sn (dot-dashed line) that is the least one. In this way, from Eqs.(5) and (6) we can see that the symmetrical potential decreases with the decrease of system density. Because the increase in mass number of system leads to the reduction in symmetrical potential, and the isospin fractionation ratio is produced mainly from symmetrical potential, so that the increase in mass number of system gives rise to a reduction in isospin fractionation ratio.

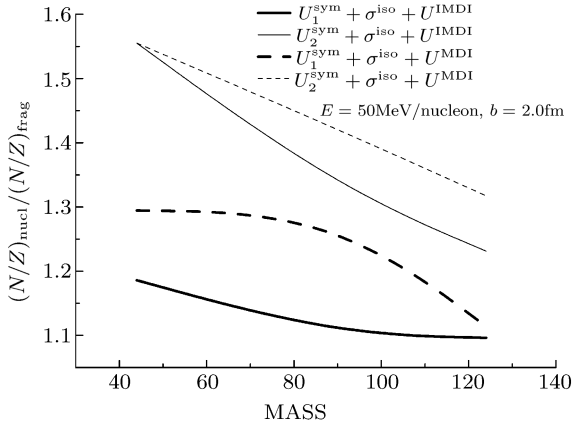


Fig.3. The variations of $(N/Z)_{\rm nucl}/(N/Z)_{\rm frag}$ at freeze-out time with system mass number at a beam energy of 50 MeV/nucleon and an impact parameter b of 2.0 fm for MDI and IMDI.

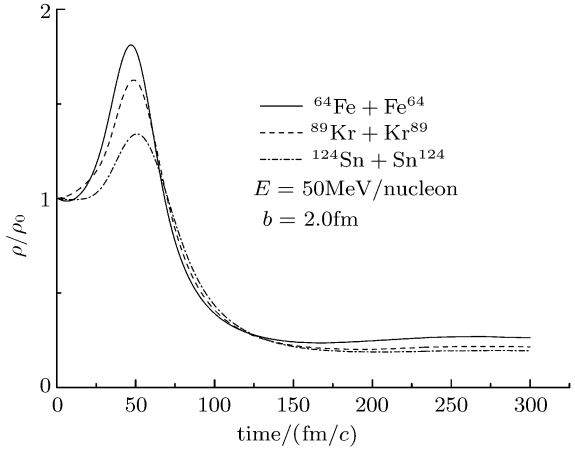


Fig.4. The variations of system density ρ/ρ_0 with collision time at a beam energy of 50 MeV/nucleon and an impact parameter of 2.0 fm for three colliding systems.

3.3. The dependences of isospin fractionation ratio $(N/Z)_{\rm nucl}/(N/Z)_{\rm frag}$ on the beam energy for MDI and IMDI

With the isospin degree of freedom in MDI included, we investigate the variation of $(N/Z)_{\rm nucl}/(N/Z)_{\rm frag}$ with beam energy. Figure 5 shows the variations of $(N/Z)_{\rm nucl}/(N/Z)_{\rm frag}$ at freeze out of time with beam energy for the reaction ^{124}Sn $+^{124}$ Sn at an impact parameter b=0.0 fm for IMDI and MDI. Clearly, IMDI causes $(N/Z)_{\rm nucl}/(N/Z)_{\rm frag}$ to significantly reduce from two dashed lines with MDI to two corresponding solid lines with IMDI for all of beam energies studied. From Fig.5 it is clear that the gap between two solid lines with IMDI is approximately the same as that between two dashed lines with MDI for $U_1^{\rm sym}$ and $U_2^{\rm sym}$. This means that the strong dependence of $(N/Z)_{\rm nucl}/(N/Z)_{\rm frag}$ on the symmetrical potential is preserved, with the isospin degree of freedom of MDI included. Figure 5 also clearly shows that the amplitude of $(N/Z)_{\rm nucl}/(N/Z)_{\rm frag}$, thus the gap between two thick lines with $U_1^{\rm sym}$ reduced by IMDI and the gap between two thin lines with $U_2^{\rm sym}$ both are enhanced with the beam energy increasing. This is due to the enhancement of the excitation energy with the increase of beam energy. In particular, the difference between $(N/Z)_{\rm nucl}/(N/Z)_{\rm frag}$ produced by different symmetry potentials, $U_1^{\rm sym}$ and $U_2^{\rm sym}$ with the same MDI and those with the same IMDI, i.e. the gap between two solid lines with IMDI and the gap between two dashed lines with MDI both increase rapidly with the increase of beam energy. This is due to the nuclear density increasing with the increase of beam energy, which enhances the symmetrical potential with the increase of nuclear density (see Eqs.(5) and (6)). Finally, it leads to the rapid increase in isospin fractionation ratio $(N/Z)_{\rm nucl}/(N/Z)_{\rm frag}$ with the increase of beam energy.

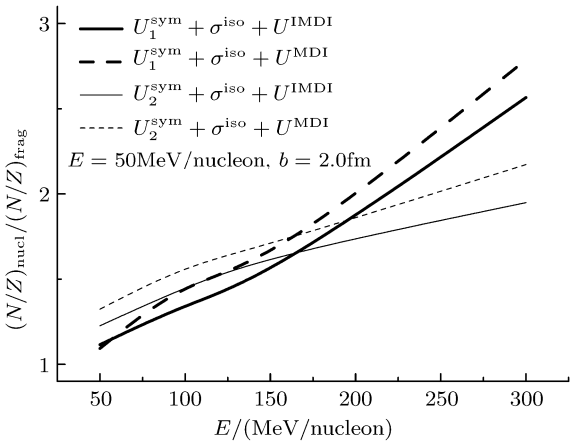


Fig.5. The variations of $(N/Z)_{\rm nucl}/(N/Z)_{\rm frag}$ for the reaction ^{124}Sn $+^{124}$ Sn with beam energy at an impact parameter $b=0.0$ fm for IMDI and MDI.

3.4. The dependences of $(N/Z)_{\rm nucl}/(N/Z)_{\rm frag}$ on the impact parameter for MDI and IMDI

We know that the observable in the nuclear reaction is sensitive to impact parameter. Figure 6 shows variations of $(N/Z)_{\rm nucl}/(N/Z)_{\rm frag}$ at freeze-out time with impact parameter b for the reaction ^{124}Sn+^{124}Sn at a beam energy of 50 MeV/nucleon for MDI and IMDI. Clearly IMDI causes $(N/Z)_{\rm nucl}/(N/Z)_{N_{\rm frag}}$ to reduce from two dashed lines with MDI to two corresponding solid lines with IMDI for all the impact parameters. However the strong dependence of $(N/Z)_{\rm nucl}/(N/Z)_{\rm frag}$ on the symmetrical potential is preserved for all the impact parameters, with the

isospin degree of freedom of MDI included, for example, the gap between two solid lines with IMDI is approximately the same in magnitude as that between two dashed lines with MDI for $U_1^{\rm sym}$ and $U_2^{\rm sym}$.

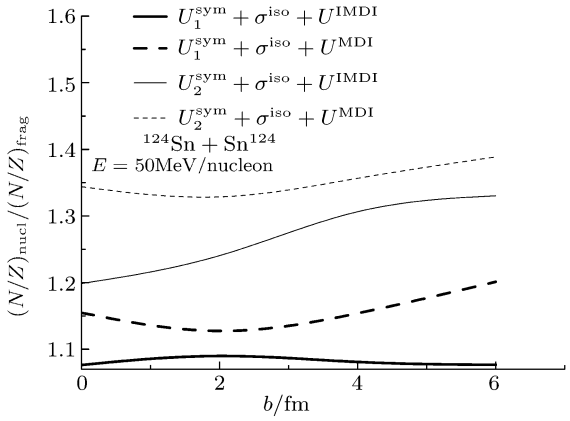


Fig.6. The variations of $(N/Z)_{\rm nucl}/(N/Z)_{\rm frag}$ at freeze-out time with impact parameter b for the reaction ^{124}Sn +^{124} Sn at a beam energy of 50 MeV/nucleon for MDI and IMDI.

Therefore, from the above results and discussion we can say that the isospin degree of freedom in MDI brings an important isospin effect to the $(N/Z)_{\rm nucl}/(N/Z)_{N_{\rm frag}}$ in the intermediate energy heavy ion collisions. This property is similar to Li's conclusion in Ref.[33]. In order to give an explanation to the reduction in $(N/Z)_{\rm nucl}/(N/Z)_{\rm frag}$ induced by IMDI, a good understanding of the variations of chemical potentials from higher to lower with the increase of nuclear density for neutrons and protons respectively, is needed. We know that the isospin fractionation is produced mainly from the chemical potential degradation. As a part of chemical potential, the isospin- and momentum-dependent potentials $U_\tau^{\rm IMDI}$ for neutrons and protons are different from each other because $U_\tau^{\rm IMDI}$ leads to the chemical potential degradations to different extents with the variation of nuclear density ρ_τ for neutrons and protons. According to the above analysis, Fig.7 shows the differences between neutron and proton potentials, $(U_{\rm n}-U_{\rm p})/2$, as a function of nuclear density ρ/ρ_0 for IMDI and MDI. Here $U_{\rm n}(U_{\rm p})\equiv U_{\rm n}(\rho,k_{\rm n},\delta)(U_p(\rho,k_{\rm p},\delta))$ is given by Eq.(12). Clearly, $U_{\rm n}^{\rm MDI}$ equals $U_{\rm p}^{\rm MDI}$ due to isospin independence for the one-body momentum-dependent potential $U_\tau^{\rm MDI}$. In this way the isospin effect in the one-body potential U_τ with isospin-independent $U^{\rm MDI}$ comes from only symmetrical potential $U^{\rm sym}$. Therefore $(U_{\rm n}-U_{\rm p})/2$ with MDI is momentum–independent of ρ/ρ_0. In this case, there is only a thick line with MDI in Fig.7. However, $(U_{\rm n}-U_{\rm p})/2$ with isospin-dependent IMDI is momentum–dependent on ρ/ρ_0 because the difference between $U_{\rm n}^{\rm IMDI}$ and $U_{\rm p}^{\rm IMDI}$ does not equal zero due to their isospin dependence. Therefore there are four thin lines with IMDI, which show the variation of $(U_{\rm n}-U_{\rm p})/2$ with nucleon momentum k as shown in Fig.7. From Fig.7 it is clear that $(U_{\rm n}-U_{\rm p})/2$ with MDI (thick solid line) is higher and steeper than $(U_{\rm n}-U_{\rm p})/2$ with IMDI (four thin lines with different k). The higher and steeper $(U_{\rm n}-U_{\rm p})/2$ with MDI leads to the faster isospin fractionation than that with $U_\tau^{\rm IMDI}$. Namely, IMDI leads $(N/Z)_{\rm nucl}/(N/Z)_{\rm frag}$ to reduce from two dashed lines with MDI to two corresponding solid lines with IMDI as shown in Fig.2, Fig.3, Fig.5 and Fig.6 for all beam energies, impact parameters and colliding systems. Therefore we can say that IMDI brings an important isospin effect to the isospin fractionation ratio for all of entrance channel conditions. However, the strong dependence of $(N/Z)_{\rm nucl}/(N/Z)_{\rm frag}$ on the symmetrical potential is preserved, with the isospin degree of freedom of MDI included for all of beam energies, impact parameters and neutron-rich colliding systems. Therefore $(N/Z)_{\rm nucl}/(N/Z)_{\rm frag}$ is still a good probe for extracting the information about the equation of state for the isospin asymmetrical nuclear matter, with the isospin degree of freedom of MDI included.

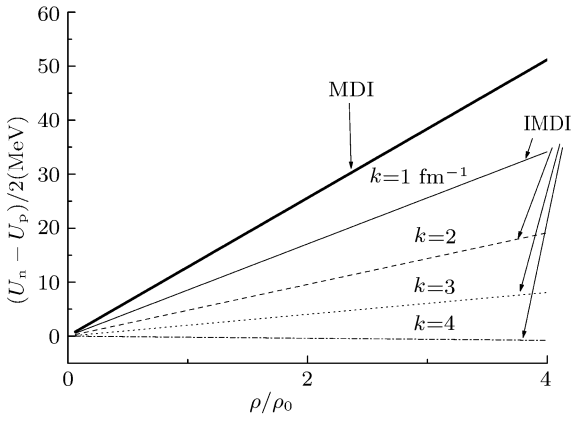


Fig.7. The differences between neutron potential and proton potential, $(U_{\rm n}-U_{\rm p})/2$, as a function of density ρ/ρ_0 for IMDI and MDI.

4. Conclusions

We obtain an isospin- and momentum-dependent interaction (IMDI) in the isospin-dependent quantum molecular dynamics model. The IMDI brings an important isospin effect to the isospin fractionation ratio in the intermediate energy heavy ion collisions because the IMDI causes a significant reduction in isospin fractionation ratio for different bean energies, impact pa-

rameters and colliding systems. However, it does not considerably change the strong dependence of isospin fractionation ratio on the symmetrical potential for all neutron-rich systems. In this case the study of the isospin dependence of MDI is important for investigating accurately the equation of state of the isospin asymmetrical matter.

References

[1] Li B A, Ko C M and Bauer W 1998 *Int. J. Mod. Phys.* E **7** 147

[2] Li B A and Udo Schröder W 2001 *Isospin Physics in Heavy-Ion Collisions at Intermediate Energies* (Nova Science Publishers, Inc New York)

[3] Li B A, Das Champak B, Das Gupta S and Gale C 2004 *Nucl. Phys.* A **735** 563

[4] Yennello S J et al 1994 *Phys. Lett.* B **321**14

[5] Pak R, Benenson W, Bjarki O, Brown J A, Hannuschke S A, Lacey R A, Li Bao-An, Nadasen A, Norbeck E, P. Pogodin5, Russ D E, Steiner M, Stone N T B, Vander Molen A M, Westfall G D, Yang L B and Yennello S J 1997 *Phys. Rev. Lett.* **78** 1022

[6] Westfall G D 1998 *Nucl. Phys.* A **630** 27c

[7] Kunde G J, Gaff S J, Gelbke C K, Glasmacher T, Huang M J, Lemmon R, Lynch W G, Manduci L, Martin L, M. B. Tsang Friedman W A, Dempsey J, Charity R J, Sobotka L G, Agnihotri D K, Djerroud B, Schr?der W U, Skulski W and Wyrozebski K 1996 *Phys. Rev. Lett.* **77** 2897

[8] Miller M, Bjarki L O, Magestro D J, Pak R, Stone N T B, Tonjes M B, Vander Molen A M, Westfall C D and Friedman W A 1999 *Phys. Rev. Lett.* **82** 1399

[9] Xu H, Tsang M B, Liu T X, Liu X D, Lynch W G, Tan W P, Vander Molen A, Verde G, Wagner A, Xi H F, Gelbke C K, Beaulieu L, Davin B, Larochelle Y, Lefort T, de Souza R T, Yanez R, Viola V E, Charity R J and Sobotka L G 2000 *Phys. Rev. Lett.* **85** 716

[10] Udo Schröder W and Toke J 2001 *Nucl. Phys.* A **681** 418c

[11] Colonna M and Matera F 2005 *Phys. Rev.* C **71** 064605

[12] Rami F, Leifels Y, de Schauenburg B, Gobbi A, Hong B, Alard J P, Andronic A, Averbeck R, Barret V, Basrak Z, Bastid N, Belyaev I, Bendarag A, Berek G, aplar R, Cindro N, Crochet P, Devismes A, Dupieux P, Delalija M, Eskef M, Finck C, Fodor Z, Folger H, Fraysse L, Genoux-Lubain A, Grigorian Y, Grishkin Y, Herrmann N, Hildenbrand K D, Kecskemeti J, Kim Y J, Koczon P, Kirejczyk M, M. Korolija, R. Kotte, M. Kowalczyk, T. Kress, R. Kutsche, Lebedev A, Lee K S, Manko V, Merlitz H, Mohren S, Moisa D, Msner J, Neubert W, Nianine A, Pelte D, Petrovici M, Pinkenburg C, Plettner C, Reisdorf W, Ritman J, Sch ü ll D, Seres Z, Sikora B, Sim K S, Simion V, Siwek-Wilczy ń ska K, Somov A, Stockmeier M R, Stoicea G, Vasiliev M, Wagner P, Winiewski K, Wohlfarth D, Yang J T, Yushmanov I and Zhilin A(FOPI Collaboration) 2000 *Phys. Rev. Lett.* **84** 1120

[13] Tsang M B, Friedman W A, Gelbke C K, Lynch W G, Verde G and Xu H S 2001 *Phys. Rev. Lett.* **86** 5023

[14] Li B A, Andrew, Sustich T and Zhang B 2001 *Phys. Rev.* C **64** 054604

[15] Li B A 2000 *Phys. Rev. Lett.* **85** 4221

[16] Li B A, Ko Che M and Ren Z Z 1997 *Phys. Rev. Lett.* **78** 1644

[17] Yennello S J, Veslesky M, Laforest R, Rowland R D, Ramakrishnan E, Ruangma A, Winchester E M and Martin E 2001 *Nucl. Phys.* A **681** 317c.

[18] Pak R, Li B A, Benenson W, Bjarki O, Brown J A, Hannuschke S A, Lacey R A, Magestro D J, Nadasen A, Norbeck E, Russ D E, Steiner M, Stone N T B, Vander Molen A M, Westfall G D, Yang L B and Yennello S J 1997 *Phys. Rev. Lett.* **78** 1026

[19] Colonna M, DiToro M, Fabbri G and Maccarone S 1998 *Phys. Rev.* C **57** 1410

[20] Liu J Y, Guo W J, Wang S J, Zuo W, Zhao Q and Yang Y F 2001 *Phys. Rev. Lett.* **86** 975

[21] Liu J Y, Zhao Q, Wang S J, Zuo W and Guo W J 2001 *Phys. Rev.* C **63** 054612

[22] Liu J Y, Guo W J, Xing Y Z, Zuo W and Lee X G 2002 *Phys. Lett.*B **540** 213

[23] Liu J Y, Xing Y Z, Guo W J, Zuo W and Lee X G 2002 *Chin. Phys. Lett.* **19** 216

[24] Liu J Y, Xing Y Z and Guo W J 2003 *Chin. Phys. Lett.* **20** 643

[25] Liu J Y, Xing Y Z and Guo W J 2003 *Chin. Phys. Lett.* **20** 8329

[26] Rong G C 2005 *Chin. Phys.* **14** 1549

[27] Guo W J, Liu J Y and Xing Y Z 2005 *Acta Phys. Sin.* **54** 3082(in Chinese)

[28] Ma Y G 2000 *Acta Phys. Sin.* **49** 654(in Chinese)

[29] Liu J Y, Guo W J, Xing Y Z and Liu H 2003 *Nucl. Phys.* A **726** 123

[30] Baran V, Colonna M and Di Toro M 2002 *Nucl. Phys.* A **703** 603

[31] Liu J Y, Guo W J, Xing Y Z, Li X G and Gao Y Y 2004 *Phys. Rev.* C **70** 034610

[32] Das C.D, Das Gupta S, Gale C and Li B A 2003 *Phys. Rev.* C **68** 014608

[33] Li B A, Das C.B, Das Gupta S and Gale C 2004 *Phys. Rev.* C **69** 011606(R)

[34] Liu J Y, Guo W J and Xing Y Z 2005 *Chin. Phys. Lett.* **22** 65

[35] Aichelin J, Rosenhauer A, Peilert G, Stoecker H and Greiner W 1987 *Phys. Rev. Lett.* **58** 1926

[36] Aichelin J, Peilert G, Bohnet A, Stocker H and Greiner W 1988 *Phys. Rev.* C **37** 2451

[37] Reinhard P G 2000 *Computational Nuclear Physics* Vol.1(Springer, Berlin) pp.28-50

[38] Klakow D, Welke G and Bauer W 1993 *Phys. Rev.* C **48** 1982

[39] Alkhazov G D, Bauer T, Bertini R, Bimbot L, Bing O, Boudard A, Bruge G, Catz H, Chaumeaux A and Couvert P 1977 *Nucl. Phys.* A **280** 365

[40] Bertsch G F and Gupta S D 1988 *Phys. Rep.* **160** 1991